

Laser Photochemistry with Polarized Light in Low-Temperature Glasses

W. Köhler, W. Breinl, and J. Friedrich*

Physikalisches Institut der Universität Bayreuth, D-8580 Bayreuth, F.R.G. (Received: August 8, 1984; In Final Form: January 16, 1985)

We have investigated the bleaching of anisotropic photochemical holes in organic glasses as a function of irradiated energy and power. We show that the width of the holes depend significantly on the relative polarization and spatial arrangement of the pump and probe beam. In case of strong bleaching it is necessary to consider the influence of photoreversibility which enhances the bleaching of the polarization but slows down the concomitant broadening of the width. Some of the model calculations are compared with experimental results.

I. Introduction

Narrow bandwidth laser photochemistry in low-temperature glasses and polymers may lead to narrow spectral holes (for a review, see ref 1-3). If these holes are burnt with polarized light and if the symmetry of the photoreactive dye molecule is not too high, photoselection may result in a persistent optical anisotropy of the sample, which is confined to a very narrow spectral range on the order of a homogeneous line width around the laser frequency, ω_L . In the simplest case the distribution of burnt molecules (i.e., of the hole) is given by

$$p(\theta) \sim \cos^2 \theta$$

with θ being the angle between the exciting laser field and the dipole moment of the absorbing molecule. This photochemically induced anisotropy can be used with advantage in a variety of spectroscopic experiments with polarized light.^{4,5}

However, as burning continues, the above distribution changes due to photochemical saturation,⁶ eventually, all molecules having $\cos \theta = 1$ are bleached, while those with $\cos \theta < 1$ are much less affected by the burning process. Hence, photochemical saturation results in a loss of anisotropy as a function of burning time. For very long burning times the burnt molecules are rather described by a spherical distribution.

In this paper we model the influence of bleaching on the anisotropy and line width of photochemical holes. The model used is based on a three-level system (Figure 1) with the educt state $|E\rangle$, a photoreactive intermediate $|I\rangle$, and the photoproduct state $|P\rangle$. The influence of a fourth level is investigated separately in section III.

The model calculations are compared with some experimental results. The sample used is 1,4-dihydroxyanthraquinone (DAQ) in an EtOH/MeOH glass (3:1, v/v), whose photochemistry is described in a series of papers (for a review, see ref 3). Hole burning was either performed with a pulsed dye laser or with a CW Ar⁺ laser. The laser line width was, in both cases, smaller than 0.02 cm⁻¹. Hole detection was performed in a collinear direction to the k vector of the burning field by using a Spex monochromator (1402) followed by a glan prism. The prism was aligned either parallel or perpendicular to the burning field. The samples were immersed in liquid He either at 1.35 or at 4.2 K.

II. Basic Model of Polarization Bleaching

We consider an inhomogeneously broadened line with a frequency distribution $p_o(\Omega)$. If laser irradiation is carried out at

a frequency ω_L , the rate R of transferring a molecule with its zero phonon origin at Ω into the photoproduct state $|P\rangle$ is calculated from the optical theorem as

$$R(\Omega, \omega_L) = \sigma \alpha \phi I / \hbar \omega_L Z(\omega_L - \Omega) \cos^2 \theta \quad (1)$$

$$\equiv K(\omega_L, \Omega) \cos^2 \theta$$

σ is the absorption cross section integrated over the homogeneous line shape, I the laser intensity, α the Debye-Waller factor, and ϕ the photochemical yield. $Z(\omega_L - \Omega)$ is the normalized zero phonon line shape function, usually a Lorentzian with a homogeneous width γ .⁶ If photochemical bleaching occurs for a time τ , the change of the relative number of molecules absorbing at Ω is calculated in the simplest way, by a first-order rate equation:⁷

$$p_r(\omega_L, \Omega, \theta) = p_o(\Omega) \exp[-K(\omega_L, \Omega)(\cos^2 \theta)\tau] \quad (2)$$

Equation 2 describes a hole in the population $p(\Omega)$ around the laser frequency ω_L . The hole is detected by scanning the burnt distribution (2) with a low-intensity beam. Hence, the observed spectral features are given by a convolution of $p_r(\omega_L, \Omega)$ with the zero phonon line shape $Z(\omega - \Omega)$.^{3,6} Since we can detect the hole either with the scanning field parallel or perpendicular to the burning field, we obtain two hole spectra, L_{\parallel} and L_{\perp} , respectively:

$$L_{\parallel}(\omega) = \alpha \sigma \int_{-\infty}^{+\infty} d\Omega p_o(\Omega) Z(\omega - \Omega) \{ [1 - \exp[-K(\omega_L, \Omega) \times (\cos^2 \theta)\tau]] \cos^2 \theta \} \quad (3a)$$

$$L_{\perp}(\omega) = \alpha \sigma \int_{-\infty}^{+\infty} d\Omega p_o(\Omega) Z(\omega - \Omega) \{ [1 - \exp[-K(\omega_L, \Omega) \times (\cos^2 \theta)\tau]] \sin^2 \theta \sin^2 \varphi \} \quad (3b)$$

Brackets indicate averaging over the unit sphere. It is interesting for comparison, to calculate the hole spectrum for an unpolarized burning field. In this case, eq 1 changes to

$$R(\omega_L, \Omega) = K(\omega_L, \Omega) \sin^2 \delta$$

with δ being now the angle between the transition dipole moment and the wave vector \vec{k} of the laser field. Accordingly, the unpolarized absorption is given by

$$L_o(\omega) = \alpha \sigma \int_{-\infty}^{+\infty} d\Omega p_o(\Omega) Z(\omega - \Omega) \{ [1 - \exp[-K(\omega_L, \Omega) \times (\sin^2 \delta)\tau]] \sin^2 \delta \} \quad (3c)$$

Equations 3a, 3b, and 3c allow for an evaluation of the optical line widths, $\Gamma_{\parallel}(\tau)$, $\Gamma_{\perp}(\tau)$, and $\Gamma_o(\tau)$, and of the degree of polarization $\rho(\tau, \omega)$ of the burnt hole

$$\rho(\tau, \omega) = \frac{L_{\parallel}(\tau, \omega) - L_{\perp}(\tau, \omega)}{L_{\parallel}(\tau, \omega) + L_{\perp}(\tau, \omega)} \quad (4)$$

(7) Voelker, S.; Macfarlane, R. M.; Genack, A. Z.; Trommsdorff, H. P.; van der Waals, J. H. *J. Chem. Phys.* 1977, 67, 1759.

(8) Dörr, F. In "Creation and Detection of the Excited State"; Lamola, A. A., Ed.; Dekker: New York, 1971.

(1) Small, G. J. In "Spectroscopy and Excitation Dynamics of Condensed Molecular Systems"; Agranovich, V. M.; Hochstrasser, R. M., Eds.; North-Holland: Amsterdam, 1983.

(2) Rebane, L. A.; Gorokhovskii, A. A.; Kikas, J. V. *Appl. Phys.* 1982, B29, 235.

(3) Friedrich, J.; Haarer, D. *Angew. Chem.* 1984, 96, 96; *Angew. Chem., Int. Ed. Engl.* 1984, 23, 113.

(4) Romagnoli, M.; Levenson, M. D.; Bjorklund, G. C. *J. Opt. Soc. Am. B: Opt. Phys.* 1984, 1, 571.

(5) Burkhalter, F. A.; Suter, G. W.; Wild, U. P.; Samoilenko, V. D.; Rasumova, N. V.; Personov, R. I. *Chem. Phys. Lett.* 1983, 94, 483.

(6) Friedrich, J.; Haarer, D. *J. Chem. Phys.* 1982, 76, 61.

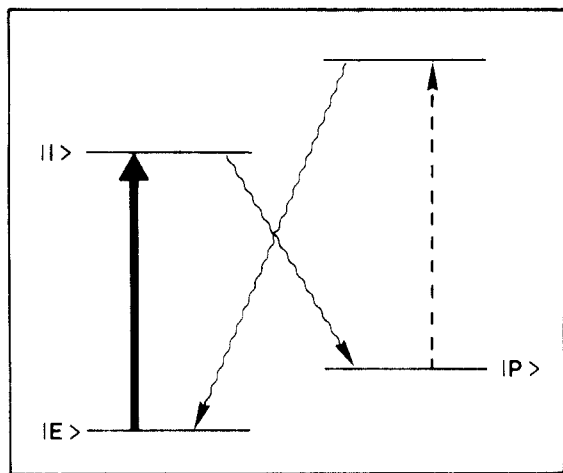


Figure 1. Level scheme used to model the polarization bleaching of photochemical holes.

as a function of burning time, τ , i.e., as a function of the state of photochemical bleaching. Γ_{\parallel} and Γ_{\perp} are the hole widths as measured with the scanning field parallel or perpendicular to the burning field. Γ_0 is the hole width in case of unpolarized excitation.

In the two limiting cases,^{3,6} $\tau \ll \tau_b$ (short burning time limit) and $\tau \gg \tau_b$ (photochemical saturation limit), an analytic evaluation is possible. Here, we have introduced a photochemical bleaching time, τ_b ,⁶ defined for the line center and for perfectly oriented molecules ($\cos \theta = 1$)

$$\tau_b^{-1} \equiv K(\Omega = \omega_L) = \frac{\alpha \sigma \phi I}{\hbar \omega_L \gamma} \quad (5)$$

with γ being the true homogeneous line width.

For $\tau \ll \tau_b$, the exponentials in eq 3a, b, c can be expanded up to second order and we get

$$\begin{aligned} \Gamma_{\parallel}(\tau) &= \gamma \left(2 + \frac{5}{14\pi} \frac{\tau}{\tau_b} \right) \\ \Gamma_{\perp}(\tau) &= \gamma \left(2 + \frac{3}{14\pi} \frac{\tau}{\tau_b} \right) \\ \Gamma_0(\tau) &= \gamma \left(2 + \frac{6}{14\pi} \frac{\tau}{\tau_b} \right) \end{aligned} \quad (6)$$

For $\tau \gg \tau_b$, $Z(\omega - \Omega)$ in eq 3 can be viewed as a δ -function as compared to a strongly saturated population hole. In this case the line width can be easily evaluated. It shows a square root dependency on the burning time.

$$\begin{aligned} \Gamma_{\parallel}(\tau) &= \gamma \left(\frac{4(2)^{1/2}}{3\pi^2} \right)^{1/3} (\tau/\tau_b)^{1/2} \\ \Gamma_{\perp}(\tau) &= \gamma \left(\frac{2(2)^{1/2}}{3\pi} \right) (\tau/\tau_b)^{1/2} \end{aligned} \quad (7)$$

For Γ_0 , a similar form is expected but an analytic representation seems not possible. Figure 2 shows a computer modeling of the three cases.

As to the degree of polarization ρ , we consider the more general case, where burning and measuring of the hole occurs in different transitions and, hence, the corresponding transition dipoles may form an angle ϵ with respect to each other. In this case the anisotropic distribution of burnt molecules has to be averaged over an appropriate Eulerian angle, ψ . Hence, $\rho_r(\omega_L, \Omega)$ (eq 2) has to be replaced by

$$\langle \rho_r(\omega_L, \Omega) \rangle_{\psi} = \rho_0(\Omega) \langle \exp[-K(\omega_L, \Omega)(\cos^2 \theta)\tau] \rangle_{\psi} \quad (8)$$

If $\tau/\tau_b \rightarrow 0$, the exponential in (8) may be approximated by a first-order expansion. Then, the averaging over ψ is straight-

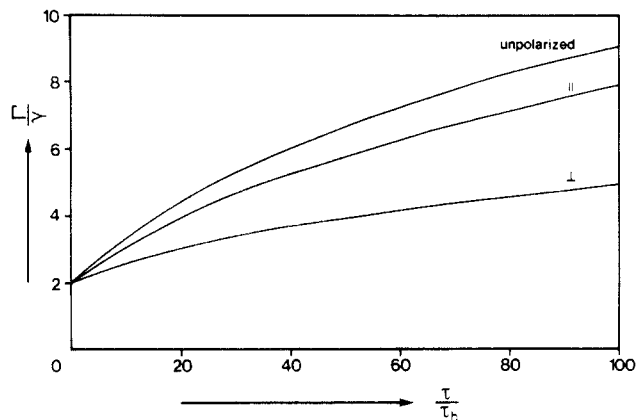


Figure 2. Hole width as a function of burning time for unpolarized and polarized excitation. In the latter case the scanning field is either parallel (Γ_{\parallel}) or perpendicular to the burning field (Γ_{\perp}).

forward and leads to the well-known Perrin formula (ref 9; see also ref 8):

$$\rho(\tau/\tau_b \rightarrow 0) \equiv \rho_0 = \frac{3 \cos^2 \epsilon - 1}{\cos^2 \epsilon + 3} \quad (9)$$

In this limiting case, ρ_0 is constant within the frequency range of the hole. It can vary between $\rho_0 = +1/2$ ($\epsilon = 0$) and $\rho_0 = -1/3$ ($\epsilon = \pi/2$). To calculate the bleaching time dependence of ρ in a first-order approximation, an expansion up to the second order of eq 8 is necessary. If we chose for simplicity $\epsilon = 0$ (in order to get rid of the ψ integration) we get

$$\rho(\tau) = \frac{1}{2} \left(1 - \frac{9}{56\pi} \frac{\tau}{\tau_b} \right), \quad \tau \ll \tau_b \quad (10)$$

that is, the bleaching of the optical anisotropy starts out in a linear fashion with a rate

$$\dot{\rho} = \frac{9}{112\pi} \frac{1}{\tau_b} \quad (11)$$

Equation 10 is calculated for the line center. However, we stress that the degree of polarization is not constant any longer but varies within the shape of the burnt hole, reflecting the different state of photochemical saturation within the optical line.

For $\tau/\tau_b \rightarrow \infty$, we again replace $Z(\omega - \Omega)$ by a δ -function, and the frequency integration can be carried out.

We find an inverse square root dependency of ρ on the burning time τ :

$$\rho(\tau/\tau_b \rightarrow \infty) = \frac{3\pi}{8(2)^{1/2}} \frac{1}{(\tau/\tau_b)^{1/2}} \quad (12)$$

Equation 12 holds for the line center (and for $\epsilon = 0$). Similar to the short burning time limit (10), the asymptotic case (12) is also frequency dependent. The loss of anisotropy is strongest for the line center and almost negligible in the wings.

Figure 3 shows the computer modeling of polarization bleaching for various frequencies within the hole. We note that the bleaching rate is largest in the short burning time limit (eq 11). Figure 4 shows a different view of the situation. Here ρ is plotted as a function of the relative hole depth (in this case L_{\parallel}). Note that the differential decrease of the anisotropy is rather small as long as the hole is shallow but gets high in case the hole gets very deep.

The bleaching of the anisotropy of spectral holes was also recently investigated by Romagnoli et al.⁴ using optical susceptibilities.

We finally stress that the degree of polarization is in principle dependent on the ratio of the homogeneous widths of both transitions. However, this dependency drops out in the two cases $\tau/\tau_b \ll 1$ and $\tau/\tau_b \gg 1$, and is only of minor importance in between these two limits.

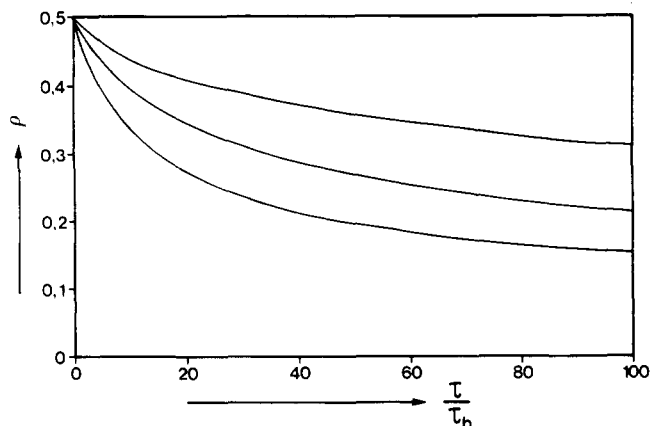


Figure 3. Bleaching of the degree of polarization as a function of burning time. The lowest curve is for the line center. The other two curves are calculated for a frequency distance of one and two half-widths, respectively.

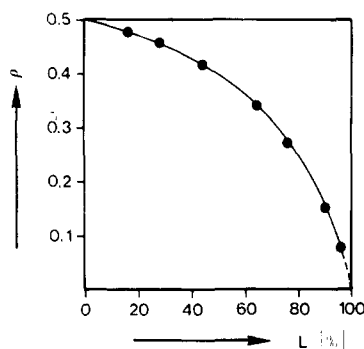


Figure 4. Degree of polarization as a function of the relative hole depth.

III. Influence of Photoreversibility on Polarization Bleaching of Persistent Holes

In the short burning time limit $\tau \ll \tau_b$, the model, outlined in section II, which is based on a three-level system, describes the experimental findings of optical bleaching quite well. For longer burning times, however, it fails to fit the experimental data. It turns out that the photochemical saturation broadening of the line width occurs on a much slower time scale than the concomitant bleaching of the polarization. To account for this discrepancy we included a fourth level (see Figure 1) in our model in order to investigate the influence of a photochemical backward reaction^{2,10} on the bleaching of the polarization and on the saturation broadening of the line width. The underlying idea is that a backward reaction enhances the bleaching of the polarization but slows down the influence of photochemical saturation on the line broadening. This latter point is obvious, since in case the reaction approaches equilibrium, the saturation broadening will stop.

Inclusion of a photoinduced backward reaction into the model results in the following rate equation:²

$$\dot{p}(\omega_L, \Omega, \theta) = -p(\omega_L, \Omega, \theta) K(\omega_L, \Omega) \cos^2 \theta + \kappa \sigma_2 \phi_2 \frac{I}{\hbar \omega_L} [p_0(\Omega) - p(\omega_L, \Omega, \theta)] \cos^2 \theta \quad (13)$$

The backward reaction is characterized by an integrated absorption cross section $\kappa \sigma_2$ into the product level (Figure 1) and a yield ϕ_2 . The factor κ is introduced to account for the fact that absorption into the product state occurs not only via zero phonon transitions, but also into phonon states. κ represents something like an inverse width averaged over the zero phonon band and the phonon tail.

In writing eq 13 it was further assumed that the transition dipole moments in the product state have the same direction as in the educt state.

The solution of eq 13 is straightforward and the calculation of photochemical saturation broadening and polarization bleaching

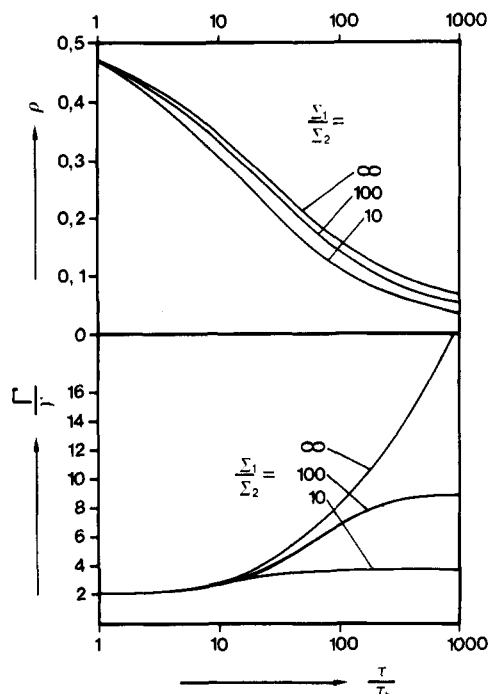


Figure 5. Photochemical saturation broadening (lower part) and polarization bleaching (upper part) of spectral holes. Σ_1/Σ_2 is the ratio of the rates of the forward (Σ_1) to the backward (Σ_2) reaction.

proceeds in a way similar to the one outlined in section II. Figure 5 shows the results: for long burning times, the influence of the backward reaction on the line width ($\Gamma_{||}$) is indeed severe (lower part of Figure 5). While the width diverges $\sim (\tau/\tau_b)^{1/2}$ in the three-level scheme, it approaches a finite value in the four-level scheme, as soon as the reaction approaches equilibrium. The magnitude of this asymptotic value of the hole width is determined by the parameter Σ_1/Σ_2 :

$$\Sigma_1 = \frac{\sigma_1 \alpha_1 \phi_1}{\hbar \omega_L \gamma_1} = \frac{1}{I \tau_{b1}} \quad (14)$$

$$\Sigma_2 = \frac{\sigma_2 \kappa \phi_2}{\hbar \omega_L}$$

The index 1 characterizes the forward reaction, 2 the backward reaction. In case $\alpha_2 \rightarrow 1$, κ approaches $1/\gamma_2$ and, hence, $\Sigma_2 \rightarrow 1/I \tau_{b2}$, i.e., Σ_1 and Σ_2 become fully symmetric.

The calculation shows that, in the short burning time limit, the line width is not affected by the backward reaction, whereas the polarization bleaching is a little bit enhanced according to

$$\rho(\tau) = \frac{1}{2} - \left(\frac{9}{112\pi} + \frac{3 \Sigma_2}{56 \Sigma_1} \right) \frac{\tau}{\tau_b} \quad (15)$$

The overall influence of photoreversibility on the bleaching of the polarization, however, is rather small (Figure 5). Figure 6 shows a different view of these findings. The hole width $\Gamma_{||}$ is plotted against the degree of polarization for various values of the parameter Σ_1/Σ_2 . As discussed above, the width tends to infinity as ρ approaches zero, if the backward reaction is neglected ($\Sigma_1/\Sigma_2 \rightarrow \infty$). On the other hand, inclusion of the reverse reaction results in a finite width, even in case the anisotropy is totally bleached. The filled circles show experimental data taken at two different temperatures, 4.2 and 1.35 K. The agreement between theory and experiment is quite satisfactory. We stress that, though the bleaching time τ_b (eq 5) may strongly increase with temperature due to a change of the homogeneous line width, γ , this influence does not show up in our calculations since reduced scales, Γ/γ and τ/τ_b , are used.

IV. Influence of Laser Power

So far our model does not contain the explicit influence of the burning power on the bleaching behavior of the optical anisotropy.

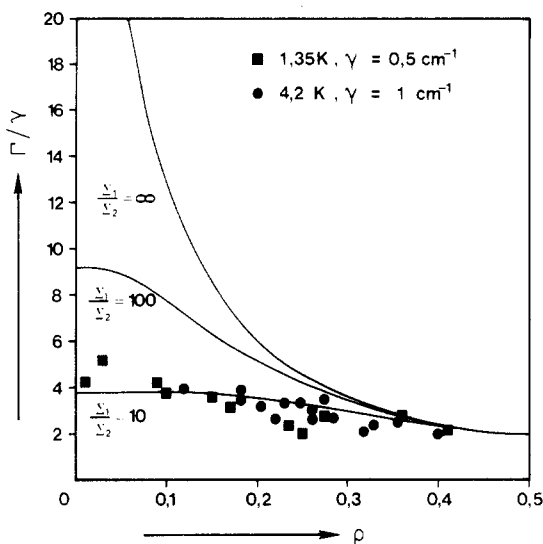


Figure 6. Hole width as a function of the degree of polarization for several values of the parameter Σ_1/Σ_2 . The squares and dots refer to experimental results.

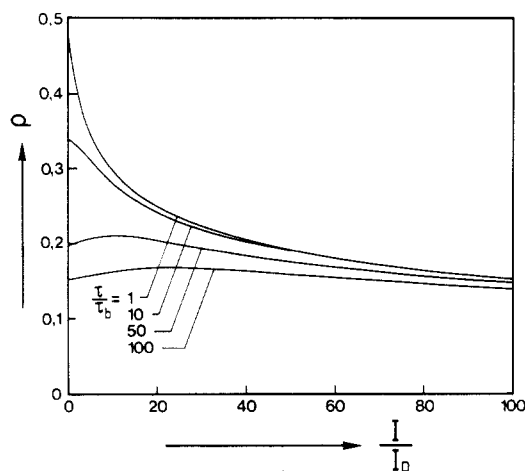


Figure 7. Degree of polarization as a function of power for various values of τ/τ_b . I_p is a critical intensity marking the onset of power broadening.

It rather depends on the product $I\tau$, i.e., on the irradiated energy. In case the photochemical yield is low, the influence of power can be simply included in our model by taking care of the fact that the homogeneous width, γ , of an optical transition changes to:¹¹

$$\gamma_p = \gamma(1 + \omega_1^2 \alpha T_1 T_2)^{1/2} \equiv \gamma(1 + I/I_p)^{1/2} \quad (16)$$

γ_p is the width of the optical transition in the presence of a strong laser field \vec{E} , which determines the Rabi frequency ω_1

$$\omega_1 = \frac{|\vec{\mu} \cdot \vec{E}| \cos \theta}{\hbar} \quad (17)$$

$\vec{\mu}$ is the molecular dipole moment.

The influence of power on the properties of the hole shows up in several ways: apart from the broadening of the hole (eq 16), strong power results in a loss of anisotropy even in the short burning time limit. This is due to the fact that, for moderately strong laser fields, saturation in the inducing transition may occur not only for molecules having $\cos \theta = 1$, but also for molecules with $\cos \theta < 1$.¹²

Figure 7 shows the fading of the degree of polarization as a function of burning power for various values of τ/τ_b (i.e., of irradiated energy). For long burning times the power dependency of the polarization becomes quite complicated.¹³ The degree of polarization even increases with increasing power. This is due

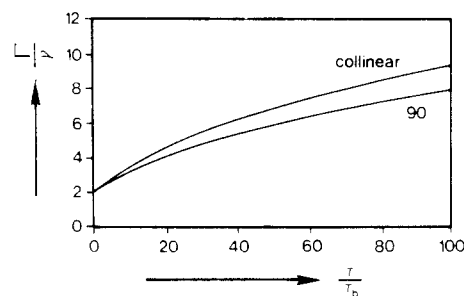


Figure 8. Hole width as a function of burning time for two different spatial configurations. Collinear: pump and probe beam have the same direction. 90°: pump and probe beam are perpendicular. Both beams are unpolarized.

to the fact that a larger line width results in a larger number of molecules that can take part in the laser photochemistry, and, hence, the bleaching occurs on a slower time scale.

One would also expect that, in isotropic solutions, the shape of the hole may depend on the laser power. In a crystal, the shape of a molecular transition is a Lorentzian with a width given by eq 16, regardless the power.¹¹ In a frozen solution, however, the Rabi frequency (eq 17) is different for differently oriented molecules and, hence, the observed line shape is rather a superposition of Lorentzians with different widths, reflecting the different state of power broadening for the various molecules which differ by their orientation angle θ .

A computer modeling, however, shows that the deviation is not severe, and a Lorentzian is still a good approximation.

V. Geometry Effects

A rather peculiar consequence of the optical anisotropy of photochemical holes is the fact that their widths (and strictly speaking their shape) may depend on the relative geometry of the detection and the excitation systems. Suppose laser irradiation is carried out with unpolarized light, resulting in an axially symmetric distribution of burnt molecules around the k vector of the exciting field. Clearly, if the hole is detected in the forward direction there is no anisotropy due to the axial symmetry. However, if detection is carried out in any other direction, e.g., perpendicular to the k vector, the hole will appear polarized, because much more molecules are burnt with their dipole axis perpendicular than parallel to the k direction. Consequently, the hole will appear narrower. Figure 8 shows computer calculations of the line width as a function of burning time for detection along the k axis and perpendicular to it, respectively. The dependence of the hole width on the spatial arrangement of the spectrometer is quite obvious.

VI. Summary

We have investigated some aspects of the bleaching of anisotropic photochemical holes in low-temperature glasses. The following results were obtained.

For low energy doses ("short burning time limit") the width of the hole varies linearly with irradiation time. The corresponding slope factor is significantly influenced by the relative polarization of pump and probe beam and is, moreover, dependent on their relative spatial arrangement. These findings have to be taken into account in case one extracts physical parameters (e.g., the photochemical yield) from the measured slope.¹⁴

For large energy doses ("photochemical saturation limit") the width evolves proportional to the square root of the burning time. Again the proportionality factor depends on the polarization of the probe and pump beam.

As for the degree of polarization, it disappears proportional to the burning time in the short burning time limit. In the photochemical saturation limit it shows an inverse square root dependency. For finite burning times the degree of polarization is no longer uniform but varies with the frequency within the hole. It

(11) Yariv, A. "Quantum Electronics", 2nd ed.; Wiley: New York, 1975.

(12) Shank, C. V.; Ippen, E. P. *Appl. Phys. Lett.* **1975**, *26*, 62.

(13) Köhler, W. Diploma Thesis, University of Bayreuth, 1984.

(14) Kador, L.; Schulte, G.; Haarer, D., to be published.

is low in the center and high in the wings.

We further found that the degree of polarization is little affected by the photoreversibility of the hole burning reaction, contrary to the width of the hole which is strongly affected. The bleaching phenomena in the width and degree of polarization of a photochemical hole show a good agreement between theory and experiment in case photoreversibility is taken into account.

Under the restrictive condition of a quasi-two-level system we investigated the influence of power on the degree of polarization in the presence of photochemical bleaching. Since strong power changes simultaneously the bleaching time (via an increase of the

width) one gets the peculiar situation that for a fixed amount of energy dose the degree of polarization may increase with increasing power.

We finally stress that the state of polarization is important with respect to several applications, most of all in the technique of frequency-modulated polarization spectroscopy⁴ but in other fields, e.g., Stark spectroscopy,⁵ as well.

Acknowledgment. We thank D. Haarer for helpful discussions. A grant from the VW-Stiftung is gratefully acknowledged.

Registry No. DAQ, 81-64-1; MeOH, 67-56-1; EtOH, 64-17-5.

Spectroscopic Characterization of Molybdenum Oxalate in Solution and on Alumina

K. Y. S. Ng, X. Zhou, and E. Gulari*

*Department of Chemical Engineering, The University of Michigan, Ann Arbor, Michigan 48109
(Received: October 30, 1984)*

The change in structure of molybdenum oxalate as a function of pH in solution and on alumina support has been investigated by Raman and FTIR spectroscopy. Both Raman and FTIR spectroscopy show that the molybdenum oxalate complex changes from a dimeric bidentate structure to a monomeric unidentate structure in solution as pH increases. Molybdenum oxalate complexes are stable when supported on alumina, as evidenced by the fact that they retain their characteristic Mo=O vibration frequency in solution. This is in sharp contrast to those samples prepared from an ammonium heptamolybdate solution. This study demonstrates the advantage of using both Raman and FTIR spectroscopy to study supported catalyst systems.

Introduction

A number of studies on the spectroscopic characterization of molybdena on alumina systems have been made in the past few years. Contradictory results were reported by different researchers probably due to different preparative procedures.¹ Such discrepancies have led to different surface models proposed for the molybdena-alumina system.² Wang and Hall² pointed out that the usual way to prepare the molybdena catalysts by incipient wetness has caused most of these complications. This is because a change of pH is unavoidable in the small volume of solution impregnated into the pores of support, and the equilibrium of the molybdate solution is pH dependent.³ Consequently, Wang and Hall² proposed a static equilibrium adsorption method to prepare a better defined catalyst. By using the equilibrium adsorption method, they showed that for pH ≤ 8 , octahedrally coordinated molybdate is the dominant species that binds to the alumina support. A small fraction of tetrahedrally coordinated molybdate species is also found in these catalysts. Cheng and Schrader⁴ investigated the effects of pH of the impregnating solution, but they did not observe a strong pH effect. All of their dried spectra indicate deposition of the Mo₇O₂₄⁶⁻ ion, even for the impregnation at pH 9 (which has mainly simple MoO₄²⁻ ions in solution). They explained the deposition of Mo₇O₂₄⁶⁻ ion as being due to the equilibrium shift when water was driven out during the drying process. Houalla et al.,⁵ on the other hand, observed a dependence of ESCA peak intensity and hydrodesulfurization activity on the pH of the impregnating solution.

The complications in the molybdena-alumina system were not only caused by the method of incipient wetness. Another underlying problem is the stability and solubility of the ammonium heptamolybdate solution (AHM), the most commonly used precursor. The relatively low solubility of the AHM and its sensitivity

to change in hydrogen and hydroxyl ion concentration undoubtedly account for the inhomogeneity of most of the impregnated catalysts. Tsigdinos et al.⁶ studied the stability and adsorption properties of molybdate solutions as a function of pH, concentration, time, temperature, and the presence of oxalate ligands. They found that the molybdenum oxalate solution has a unique adsorption behavior in that the amount adsorbed on alumina is independent of concentration. More recently, Streusand et al.⁷ studied the adsorption behavior of molybdenum oxalate in a bimetallic solution and found similar results. They further suggested that the adsorption mechanism of molybdenum oxalate onto alumina is different from that based on AHM solutions.

The purpose of this work was to characterize the molybdenum oxalate in solution and on alumina by Raman and FTIR spectroscopy. The equilibrium adsorption technique has the merit of producing more disperse and homogeneous catalysts, but it may have drawbacks in dealing with higher metal loadings and bimetallic solutions. Molybdenum oxalate is well-known to form stable complex species in aqueous solution.⁸ In this study we want to investigate whether a more stable molybdenum oxalate solution of higher buffer capacity will lead to a more homogeneous catalyst even under incipient wetness conditions.

Experimental Methods

Material and Catalyst Preparation. Molybdenum oxalate solution was prepared from molybdenum oxalate salts (Climax Molybdenum Co.) by using doubly distilled water. Solutions of higher pHs were obtained by adding ammonium hydroxide. Catalysts were prepared by the method of incipient wetness. Support material was γ -alumina (BDH Chemicals, Ltd.) with a surface area of 100 m²/g. Samples were air-dried at 110 °C for 12 h.

(1) Massoth, F. E. *Adv. Catal.* **1978**, *27*, 265.

(2) Wang, L.; Hall, W. K. *J. Catal.* **1980**, *66*, 252.

(3) Ng, K. Y. S.; Gulari, E. *Polyhedron* **1984**, *8*, 1001.

(4) Cheng, C. P.; Schrader, G. L. *J. Catal.* **1979**, *60*, 276.

(5) Houalla, M.; Kibby, C. L.; Petrakis, L.; Hercules, D. M. *J. Catal.* **1983**, *83*, 50.

(6) Tsigdinos, G. A.; Chen, H. Y.; Streusand, B. J. *Ind. Eng. Chem. Prod. Res. Dev.* **1981**, *20*, 619.

(7) Streusand, B. J.; Husby-Coupland, K. J. Report L-287-81/83; Climax Molybdenum Co.: Ann Arbor, MI, 1984.

(8) Beltran, A.; Caturla, F.; Cervilla, A.; Beltran, J. *J. Inorg. Nucl. Chem.* **1981**, *43*, 3277.